Crystal structures and spectroscopic properties of platina-β-diketones — a new mode of stacking in platinum complexes

Dirk Steinborn [a,*], Michael Gerisch [a], Tobias Hoffmann [a], Clemens Bruhn [a], Gunter Israel [b], Franz W. Müller [b]

[a] *Institut für Anorganische Chemie der Martin-Luther, Universität Halle-Wittenberg, Kurt-Mothes-Strasse 2, D-06120 Halle Saale, Germany*
[b] *Institut für Organische Chemie der Martin-Luther, Universität Halle-Wittenberg, Kurt-Mothes-Strasse 2, D-06120 Halle Saale, Germany*

Dedicated to Professor Dirk Walther on the occasion of his 60th birthday

Abstract

Platina-β-diketones $[Pt_2\{(COR)_2H\}_2(\mu\text{-Cl})_2]$ (R = Me **1a**, Et **1b**, *n*-Pent **1c**, *n*-Hex **1d**, $(CH_2)_4Ph$ **1e**) are prepared by reaction of hexachloroplatinic acid in *n*-butanol with silyl-substituted acetylenes $R'C\equiv CSiMe_3$ (R′ = R–CH$_2$). Complexes **1** are characterized by NMR, IR and UV–vis spectroscopies. The crystal structures of complexes **1a**, **b**, **e** reveal discrete dinuclear molecules linked via Pt···Pt interactions [$d(Pt\cdots Pt)$ = 3.318(1)–3.352(1) Å] in such a way that polymeric chain-like structures are formed. These complexes exhibit only an emission in the solid state (λ_{max} 555 nm) that is ascribed to a d^8–d^8 electronic excited state. No emission is observed in solution. The distinct differences in the absorption and emission spectra in solution and in the solid state, as well as the lack of photoconductivity, are ascribed to the columnar structures in the solid state with the mode of stacking of the platinum centers with alternating Pt···Pt interactions and Pt–Cl–Pt bridges. © 2000 Elsevier Science S.A. All rights reserved.

Keywords: Platinum; Closed-shell interactions; Crystal structure; Emission spectroscopy

1. Introduction

It is well known that square-planar platinum complexes have the tendency to stack in the solid state via closed-shell interactions [1,2]. In fact, both absorption and emission spectra of platinum(II) complexes are strongly dependent on intermolecular stacking interactions in solution and in the solid state [3]. We recently reported the synthesis of platina-β-diketones $[Pt_2\{(COR)_2H\}_2(\mu\text{-Cl})_2]$ (R = Me **1a**, Et **1b**) [4]. These are new representatives of the well-known metalla-β-diketones, but contrary to Lukehart's complexes $[M\{(COR)_2H\}L_x]$ (M = Mn, Re, Fe, …; L = CO, Cp)

[5], they are electronically unsaturated complexes (16 valence electrons) with a kinetically labile ligand sphere. During our ongoing studies, we observed that complexes **1** are intensely yellow in their solid state but their solutions are only light yellow. In order to gain insight into the relationship between crystal packing and electronic structure, we synthesized new platina-β-diketones and studied their spectroscopic properties, in particular the electronic spectra, both in solution and in the solid state.
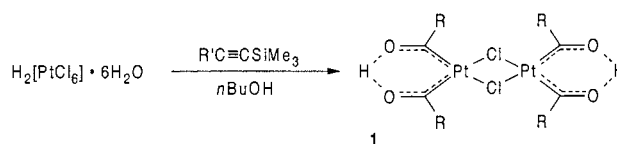
Scheme 1. R = Me **1a**, Et **1b**, *n*-Pent **1c**, *n*-Hex **1d**, $(CH_2)_4Ph$ **1e**; R′ = R–CH$_2$.

* Corresponding author. Tel.: +49-345-5525620; fax: +49-345-5527028.

E-mail address: steinborn@chemie.uni-halle.de (D. Steinborn)

Table 1
Selected spectroscopic data and properties for [Pt$_2${(COR)$_2$H}$_2$(μ-Cl)$_2$] (**1a**–**1e**)

	R	m.p.(dec.) (°C)	Δm [a] in % observed (calculated)	δ(CO) (ppm)	^1J(Pt, C) (Hz)	v(CO) (cm^{-1})	v(PtCl) (cm^{-1})
1a	Me	183	40.4 (38.6)	228.1	1457	1548	238
1b	Et	176	47.5 (43.6)	231.0	1459	1539	251
1c	n-Pent	159	56.6 (54.6)	231.5	1469	1548	264
1d	n-Hex	86 [b]	57.0 (57.4)	231.8	1447	1550	260
1	(CH$_2$)$_4$Ph	156	67.8 (67.8)	231.0	1462	1549	269

[a] **1e** mass loss after heating to 400°C; calculated values for Pt as residue.
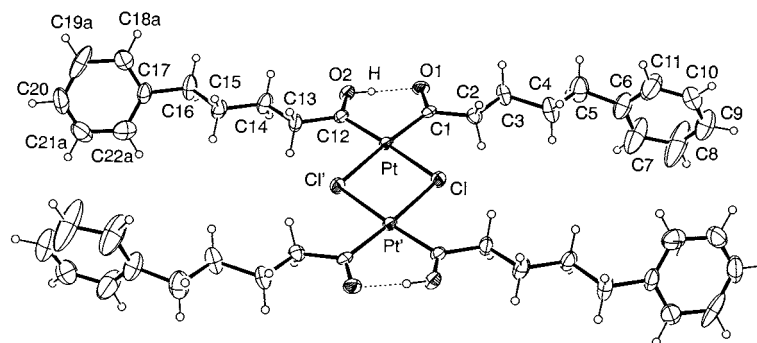[b] Decomposition temperature 161°C.

Fig. 1. ORTEP-III plot [17] of [Pt$_2${[CO(CH$_2$)$_4$Ph]$_2$H}$_2$(μ-Cl)$_2$] (**1e**), displaying atom numbering (displacement ellipsoids at 30% probability). Only one position of the disordered phenyl ring C(17)–C(20) is shown.

2. Results and discussion

2.1. Synthesis and characterization

Hexachloroplatinic acid reacts with the trimethylsilyl-substituted alkynes R′C≡CSiMe$_3$ (R′ = n-Bu, n-Pent, (CH$_2$)$_3$Ph) in n-butanol via H[PtCl$_3$(η^2-CH$_2$=CHEt)] [6] as intermediate to yield the novel platina-β-diketones [Pt$_2${(COR)$_2$H}$_2$(μ-Cl)$_2$] (R = n-Pent **1c**, n-Hex **1d**, (CH$_2$)$_4$Ph **1e**) (Scheme 1). Complexes **1** are isolated as yellow crystals in moderate to good yields (44–81%). Analogous reactions with PhC≡CSiMe$_3$, ClCH$_2$C≡CSiMe$_3$ or Me$_3$CC≡CSiMe$_3$ gave mixtures of products where no identifiable compounds could be isolated. All platina-β-diketones **1** are moderately air sensitive. Solutions of **1** in acetone, chloroform, or methylene chloride decompose at room temperature under argon within a few days.

Complexes **1** exhibit remarkable thermal stability (Table 1); they melt under decomposition between 156 and 183°C, except for **1d** which melts already at 86°C. Heating the complexes up to 400°C results in formation of platinum metal as demonstrated by thermogravimetric analysis.

There are no remarkable differences between the NMR and IR spectroscopic data of **1c**−**e** and those of **1a**−**b** (Table 1). In all five complexes ^{1}H- and ^{13}C-NMR spectra reveal the equivalence of all four COR groups. The chemical shifts of the carbonyl carbon atoms (228.1–231.8 ppm) and the ^1J(Pt, C) coupling constants (1447–1469 Hz) do not depend strongly on the substituent R. The proton resonances of the hydrogen atoms involved in the O–H···O hydrogen bridges could not be observed due to line broadening. The v(PtCl) and v(CO) vibrations are at 238–269 and 1539–1550 cm^{-1}, respectively.

2.2. Molecular and crystal structure

The molecular structure of complex **1e** is shown in Fig. 1. Table 2 contains selected atom distances and

Table 2
Selected interatomic distances (Å) and angles (°) for [Pt$_2${[CO(CH$_2$)$_4$Ph]$_2$H}$_2$(μ-Cl)$_2$] (**1e**) [a]

Bond distances			
Pt–C(1)	1.967(9)	C(1)–O(1)	1.24(1)
Pt–C(12)	1.964(8)	C(12)–O(2)	1.24(1)
Pt–Cl	2.452(2)	O(1)···O(2)	2.391(9)
Pt–Cl′	2.444(2)	Pt···Pt″	3.3176(8)
Bond angles			
C(1)–Pt–C(12)	90.8(4)	Cl–Pt–Cl′	79.52(7)
C(1)–Pt–Cl	94.8(3)	Pt–Cl–Pt′	100.48(7)
C(1)–Pt–Cl′	174.1(3)	Pt–C(1)–O(1)	125.1(6)
C(12)–Pt–Cl	173.6(3)	Pt–C(12)–O(2)	124.7(6)
C(12)–Pt–Cl′	94.8(3)		

[a] Symmetry code: ′, −x, −y+1, −z+1; ″, −x, −y, −z+1.
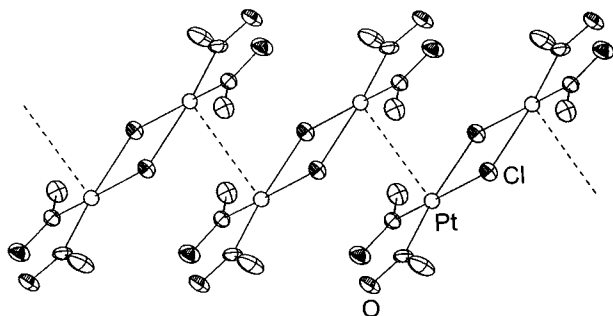
Fig. 2. Chain-like structure (parallel crystallographic *a* axis) of [Pt$_2$\{(COMe)$_2$H\}$_2$(μ-Cl)$_2$] (**1a**).

bond angles. The dinuclear molecule exhibits crystallographically imposed C_i symmetry. Obviously due to great flexibility of the 4-phenylbutyl groups in the packing, the phenyl group C(17)–C(22) is disordered over two positions with equal probability [angle between the two disordered phenyl ring planes: 47(2)°]. The platina-β-diketone unit is nearly planar [greatest deviation: 0.043(9) Å for C(12)]. The Pt–C bond lengths in **1e** [1.967(9)/1.964(8) Å] and the C–O bond lengths [1.24(1)/1.24(1) Å] are in each case equivalent within 1σ and do not differ significantly from those in the platina-β-diketones **1a** and **1b** [d(Pt–C) = 1.95(1)–1.97(1) Å; d(C–O) = 1.23(1)–1.26(1) Å] [4]. The O···O distance in the intramolecular O···H···O hydrogen bond is 2.391(9) Å and thus, in the range of those in complexes **1a** and **1b** [**1a**, 2.37(1); **1b**, 2.40(1) Å] and of those in other complexes with platina-β-diketone units [2.28(4)–2.419(8) Å] [7,8]. Apart from these very strong hydrogen bonds, there are weak C–H···Cl hydrogen-bond interactions [9] between α-C–H hydrogens of 4-phenylbutyl substituents and μ-chloro ligands [C(2)–H···Cl: d(C···Cl) = 3.12(1) Å, ∠(C–H···Cl) 105.2°; C(13)–H···Cl′: d(C···Cl′) = 3.16(1) Å, ∠(C–H···Cl) 105.8°].

The most noticeable feature of the crystal structures of complexes **1a**, **1b** and **1e** is the stacking of the discrete molecules of **1** by closed-shell d^8–d^8 interactions [2] forming a polymeric chain-like and ladder-like structure, as is shown for complex **1a** in Fig. 2. The Pt···Pt distances (Table 3) range from 3.318(1) to

3.352(1) Å. The central Pt···Pt distances in tetranuclear platina-β-diketonates of platina-β-diketones [\{XX′Pt(μ-COMe)$_2$Pt[(COMe)$_2$H]\}$_2$]^n (X/X′ = Cl/Cl, $n = 2-$; X/X′ = PhNH$_2$/Cl, $n = 0$; X/X′ = bpy, $n = 2+$), which can be regarded as organometallic analogues of platinum blue complexes, are significantly shorter [3.094(1)–3.186(2) Å] [7]. All these values are within the range of Pt···Pt distances in platinum(II) complexes with columnar structures (3.09–3.60 Å) [1,10].

Thus, the crystals are threaded by chains which are parallel to the crystallographic *a* (**1a**, **1b**) and *b* (**1e**) axes, respectively. The chains in complex **1a** are related by the space group ($P2_1/n$) glide plane and therefore have different orientations. In complexes **1b** and **1e** all chains are oriented in the same direction (Fig. 3).

2.3. Electronic spectra

The solution spectra of platina-β-diketones **1** (Table 3) show no absorption above 400 nm. All compounds exhibit an intense absorption centered at 234–244 nm and a second less intense one at about 305 nm with a shoulder at about 338 nm. Two of these bands can be attributed to the strongly allowed π–π* (234–244 nm) and the corresponding weak n–π* transitions (338 nm) of the platina-β-diketone moiety. The absorption band centered at 305 nm may arise from the lowest ligand field singlet-triplet transition of the Pt(II) complex [11].

Aggregation in methylene chloride solution does not take place as demonstrated by utilizing UV–vis measurements of **1a** at variable concentrations ranging from 1.9×10^{-5} M to a saturated solution (1.9×10^{-2} M). All absorption bands follow Beer's law. This is supported by the fact that a molar mass determination of complex **1a** reveals dinuclear units in chloroform solution (found: 641.9 g mol^{-1}; calculated for [Pt$_2$\{(COMe)$_2$H\}$_2$(μ-Cl)$_2$]: 635.3 g mol^{-1}).

In the solid state all platina-β-diketones **1** have only one broad absorption band at 412–448 nm (Table 3). This maximum absorption corresponds to the Pt···Pt distance 3.32–3.35 Å in the stacks, as was found for many platinum complexes with metal–metal interaction [1,12]. Emission after electronic excitation of platina-β-

Table 3
Interatomic Pt···Pt distances and photophysical data for [Pt$_2$\{(COR)$_2$H\}$_2$(μ-Cl)$_2$] (**1a–1e**)

	R	d(Pt···Pt) (Å)	Absorption (solution) λ_{max} (nm) (ϵ in 10^4 M^{-1} cm^{-1})	Absorption (solid state) λ_{max} (nm)	Emission (solid state) [a] λ_{max} (nm) [b]
1a	Me	3.352(1)	244 (2.36), 305 (1.50), 334 (1.0)	412	555 (57)
1b	Et	3.338(1)	238 (1.19), 306 (0.56), 337 (0.4)	420	555 (7)
1c	*n*-Pent		234 (0.95), 302 (0.33), 342 (0.2)	412	555 (14)
1d	*n*-Hex		242 (1.84), 308 (0.94), 342 (0.6)	448	555 (16)
1e	(CH$_2$)$_4$Ph	3.318(1)	242 (1.74), 308 (1.27), 337 (0.9)	412	555 (15)

[a] λ_{exc} = 389 nm.
[b] Intensity (arbitrary units) in parentheses.

Fig. 4. Emission spectra of $[Pt_2\{(COMe)_2H\}_2(\mu\text{-}Cl)_2]$ (**1a**) (a) in solid state and (b) in CH_2Cl_2 solution at room temperature, $\lambda_{exc} = 389$ nm.

diketones **1** can be observed in the solid state, whereas in solution no emission was found (Fig. 4). This result strongly favors a ligand field (d^8–d^8) electronic excited state as emissive state of the dimers (via Pt···Pt interactions) of the dimeric complexes **1** (via Pt–Cl–Pt bridges) [11,13]. As stated above, no aggregation and hence no Pt···Pt interaction necessary for the formation of emissive states takes place in solution. The lifetime $\tau = 308$ ns of the emission (**1a**, room temperature; $\lambda_{exc} = 478$ nm, conventional laser single photon counting technique) indicates a triplet–singlet transition.

lt has been shown in Fig. 2 that molecules of platina-β-diketones **1** are linked by platinum–platinum interactions forming polymer chains. Such interactions are favorable for thermal or photoconductivity along the stacking axis of the solid as is known from $[Pt(CN)_4]^{2-}$ complexes [1,12]. However, time-resolved photo–e.m.f. measurements [14] using solid **1a** did not show any transient or long living photo–e.m.f. signals. This indicates that **1a** does not behave as a photo-conductor forming free electrons and holes after absorption of light. This lack of any photoconductivity may be attributed to the formation of only dimers in respect to the Pt···Pt interaction. Charge transport through the Pt–Cl–Pt unit seems to be very limited. This alternating bridging (Pt···Pt and Pt–Cl–Pt) of the platinum centers in the solid-state structures of platina-β-diketones represents a new mode of linkage in platinum complexes and is the decisive difference from other platinum(II) complexes with columnar structures built up of ···Pt···Pt···Pt··· chains.

3. Experimental

All preparations were carried out under argon using standard Schlenk techniques. Methylene chloride was dried over CaH_2 and distilled prior to use. The trimethylsilyl-substituted acetylenes were prepared by reaction the corresponding terminal alkyne with *n*-butyllithium and trimethylchlorosilane [15], except 1-
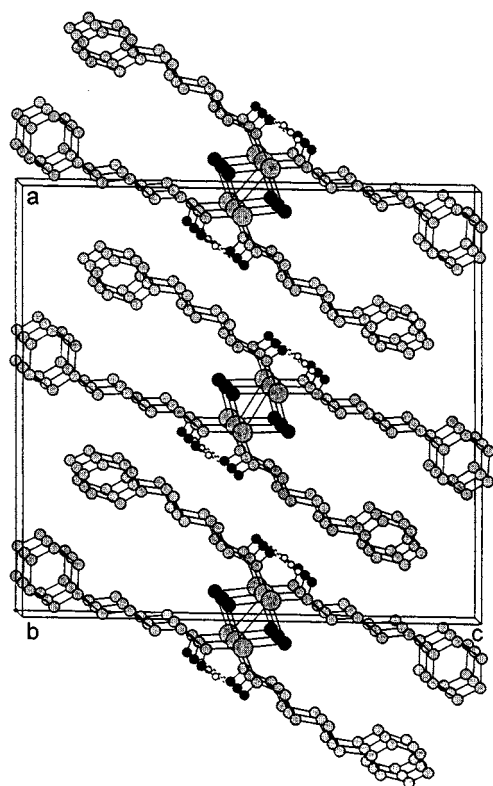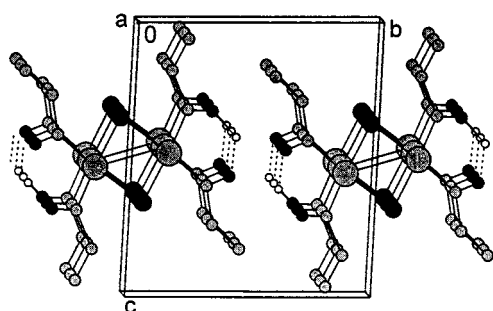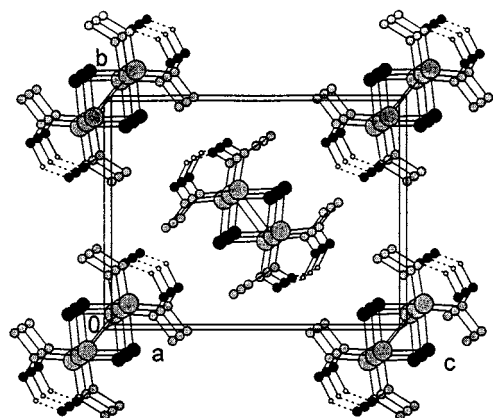

Fig. 3. Orientation of chains in crystals of platina-β-diketones $[Pt_2\{(COR)_2H\}_2(\mu\text{-}Cl)_2]$ (from top to bottom: R = Me **1a**, Et **1b**, $(CH_2)_4Ph$ **1e**); projections along the chain directions.

Table 4
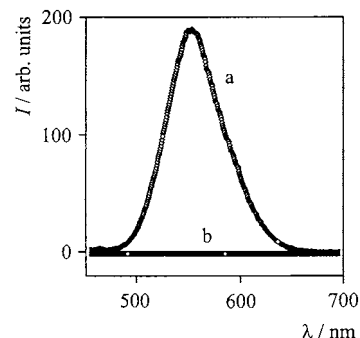Crystal data and structure refinement details for compound **1e**

Formula	$C_{44}H_{54}Cl_2O_4Pt_2$
M_r	1107.95
Temperature (K)	220(2)
Crystal system/space group	Monoclinic/$P2_1/a$ (no. 14)
a (Å)	19.784(4)
b (Å)	5.0107(6)
c (Å)	21.110(4)
β (°)	91.04(2)
V (Å^3)	2092.3(6)
Z	2
Crystal dimensions (mm)	$0.13 \times 0.10 \times 0.06$
$\rho_{calc.}$ (g cm^{-3})	1.759
μ(Mo–K$_\alpha$) (mm^{-1})	6.847
$F(000)$	1080
Scan range (°)	$2.29 < \theta < 24.92$
Reciprocal lattice segments h, k, l	$-22 \rightarrow 23$, $-5 \rightarrow 5$, $-24 \rightarrow 24$
Reflections collected	11 447
Independent reflections	3598 ($R_{int} = 0.0784$)
Data/restraints/parameters	3598/0/275
Goodness-of-fit on F^2	1.056
Final R, $[I > 2\sigma(I)]$	$R_1 = 0.0460$, $wR_2 = 0.1142$
R, all data	$R_1 = 0.0586$, $wR_2 = 0.1200$
Largest difference peak and hole (e Å^{-3})	2.996 and -1.508

trimethylsilylprop-1-yne, which was purchased from Fluka and used as received. The platina-β-diketones [Pt$_2${(COR)$_2$H}$_2$(μ-Cl)$_2$] (R = Me **1a**, Et **1b**) were obtained according to the literature [4]. ^{1}H- and ^{13}C-NMR spectra were recorded on Varian Gemini 200 and Varian VXR 400 NMR spectrometers. Chemical shifts are relative to CHDCl$_2$ (δ 5.32) and CD_2Cl$_2$ (δ 53.8) as internal references. IR spectra were recorded on a Galaxy FT-IR spectrometer Mattson 5000 using CsBr pellets. Electronic absorption spectra were obtained on a Perkin–Elmer UV–vis/NIR (solid state) and on a Carl-Zeiss MCS 400 spectrometer (solution). Emission measurements were taken on a Perkin–Elmer LS 50B spectrometer in a right-angle (solution) or front-surface (microcrystalline powder) arrangement. Spectra were collected using 1-cm quartz fluorescence cells with dry methylene chloride as solvent. Photo–e.m.f. measurements were performed using a capacitor circuit with an optically transparent front electrode (NESA-glass) and a 800 kW nitrogen pumped dye laser from Laser Technique, Berlin ($\lambda_{exc.} = 469$ nm, 1.4×10^{13} quanta per flash, $t_{1/2} = 0.5$ ns) [14]. Thermoanalytical measurements were recorded on Netzsch STA 409C with a heating rate of 10 K min^{-1}. For the molecular mass determination a vapor-pressure osmometer A0280 (Knauer, Berlin) was used.

3.1. Synthesis of [Pt$_2${(COR)$_2$H}$_2$(μ-Cl)$_2$] (1)

A solution of hexachloroplatinic acid, H$_2$[PtCl$_6$]· 6H$_2$O, (0.51 g, 1.05 mmol) in n-butanol (3 cm^3, 33

mmol) was kept at 100°C for 3 h. Then the corresponding trimethylsilyl-substituted acetylene (15 mmol) was added at room temperature. On standing overnight, intensely yellow needles of **1** were formed, which were washed with diethyl ether (10 cm^3) and dried in vacuo.

3.1.1. R = n-Pent (1c)

Yield: 272 mg (65%). m.p. (dec.) 159°C. IR (CsBr): ν(OHO) 1634, ν(CO) 1548, ν(PtCl) 264 cm^{-1}. ^{1}H-NMR (400 MHz, CDCl$_3$): $\delta = 0.89$ (t, 12H, CH_3), 1.29 (m, 16H, $2 \times$ CH_2), 1.67 (m, 8H, CH_2), 2.79 (t, 8H, CH_2), resonance for OHO not observed. ^{13}C-NMR (101 MHz, CDCl$_3$): $\delta = 14.1$ (CH_3), 22.5, 24.9, 31.4 ($3 \times$ CH_2), 51.3 (s + d, ^2J(PtC) = 148 Hz, CH_2), 231.5 (s + d, ^1J(PtC) = 1469 Hz, CO). C$_{24}$H$_{46}$Cl$_2$O$_4$Pt$_2$ (859.72): Anal. Calc. C, 33.53; H, 5.39; found: C, 33.16; H, 5.24%.

3.1.2. R = n-Hex (1d)

Yield: 212 mg (44%). m.p. (dec.): 161°C. IR (CsBr): ν(OHO) 1646, 1636 ν(CO) 1550, ν(PtCl) 260 cm^{-1}. ^{1}H-NMR (400 MHz, CDCl$_3$): $\delta = 0.85$ (t, 12H, CH_3), 1.26 (m, 24H, $3 \times$ CH_2), 1.62 (m, 8H, CH_2), 2.76 (t, 8H, CH_2), resonance for OHO not observed. ^{13}C-NMR (101 MHz, CDCl$_3$): $\delta = 13.9$ (CH_3), 22.6, 25.2, 28.9, 31.6 ($4 \times$ CH_2), 51.4 (s + d, ^2J(PtC) = 143 Hz, CH_2), 231.8 (s + d, ^1J(PtC) = 1447 Hz, CO). C$_{28}$H$_{54}$Cl$_2$O$_4$Pt$_2$ (915.83): Anal. Calc. C, 36.72; H, 5.94; Cl, 7.74; found: C, 36.13; H, 5.66; Cl, 7.58%.

3.1.3. R=(CH$_2$)$_4$Ph (1e)

Yield: 942 mg (81%). m.p. (dec.): 156°C. IR (CsBr): ν(OHO) 1636 ν(CO) 1549, ν(PtCl) 269 cm^{-1}. ^{1}H-NMR (400 MHz, CDCl$_3$): $\delta = 1.62$ (m, 8H, CH_2), 1.69 (m, 8H, CH_2), 2.60 (t, 8H, CH_2), 2.81 (t, 8H, CH_2), 7.20 (m, 20H, CH), resonance for OHO not observed. ^{13}C-NMR (101 MHz, CDCl$_3$): $\delta = 24.5$, 30.6, 35.5 ($3 \times$ CH_2), 50.8 (s + d, ^2J(PtC) = 143 Hz, CH_2), 125.9 (p-CH), 128.39/128.41 (o/m-CH), 142.1 (i-CH), 231.0 (s + d, ^1J(PtC) = 1462 Hz, CO). C$_{44}$H$_{54}$Cl$_2$O$_4$Pt$_2$ (1108.01): Anal. Calc. C, 47.70; H, 4.91; Cl, 6.40; found: C, 47.67; H, 4.84; Cl, 6.73%.

3.2. Crystal-structure determination of complex 1e

Intensity data were collected on a Stoe IPDS diffractometer with Mo–K$_\alpha$ radiation (0.71073 Å, graphite monochromator). A summary of the crystallographic data, the data-collection parameters, and the refinement parameters is given in Table 4. Absorption correction was carried out numerically ($T_{min.}/T_{max.}$ 0.26/0.29). The structure was solved by direct methods with SHELXS-86 [16] and refined using full-matrix least-squares routines against F^2 with SHELXL-93 [16]. Non-hydrogen atoms were refined with anisotropic displacement parameters. The H-atoms were added to the model in their calcu-

lated positions and refined isotropically, except for the bridging H-atom, which was found in the difference Fourier map. Obviously due to the great flexibility in the packing, the phenyl ring C(17)–C(22) is disordered over two positions which are occupied with the same probability. The other phenyl ring C(6)–C(11) shows large displacement ellipsoids only.

4. Supplementary material

Crystallographic data (excluding structure factors) for **1e** have been deposited at the Cambridge Crystallographic Data Center as supplementary publication no. CCDC 133209. Copies of the data can be obtained free of charge on application to CCDC, 12 Union Road, Cambridge, CB2, 1EZ, UK (Fax: +44-1223-336033; e-mail: deposit@ccdc.cam.ac.uk).

Acknowledgements

References

[1] (a) K. Krogmann, Angew. Chem. 81 (1969) 10. (b) J.S. Miller, A.J. Epstein, Prog. Inorg. Chem. 20 (1976) 1. (c) J.M. Williams, Adv. Inorg. Radiochem. 26 (1983) 235.

[2] P. Pyykkö, Chem. Rev. 97 (1997) 597.

[3] (a) W.B. Connick, L.M. Henling, R.E. Marsh, H.B. Gray, Inorg. Chem. 35 (1996) 6261. (b) C.-M. Che, V.W.-W. Yam, W.-T. Wong, T.-F. Lai, Inorg. Chem. 28 (1989) 2908. (c) C.-M. Che, L.-Y. He, C.-K. Poon, T.C.W. Mak, Inorg. Chem. 28 (1989) 3081. (d) J. Biedermann, G. Gliemann, U. Klement, K.-J. Range, M. Zabel, Inorg. Chem. 29 (1990) 1884. (e) H.-K. Yip, C.-M. Che, Z.-Y. Zhou, T.C.W. Mak, J. Chem. Soc. Chem. Commun. (1992) 1369. (f) B. Pomarède, B. Garreau, I. Malfant, L. Valade, P. Cassoux, J.-P. Legros, A. Audouard, L. Brossard, J.-P. Ulmet, M.-L. Doublet, E. Canadell, Inorg. Chem. 33 (1994) 3401. (g) J.A. Bailey, M.G. Hill, R.E. Marsh, V.M. Miskowski, W.P. Schaefer, H.B. Gray, Inorg. Chem. 34 (1995) 4591. (h) M. Kato, K. Sasano, C. Kosuge, M. Yamazaki, S. Yano, M. Kimura, Inorg. Chem. 35 (1996) 116. (i) W. Paw, R.J. Lachicotte, R. Eisenberg, Inorg. Chem. 37 (1998) 4139.

[4] (a) D. Steinborn, M. Gerisch, K. Merzweiler, K. Schenzel, K. Pelz, H. Bögel, J. Magull, Organometallics 15 (1996) 2454. (b) F.W. Heinemann, M. Gerisch, D. Steinborn, Z. Kristallogr. 212 (1997) 181.

[5] (a) C.M. Lukehart, Acc. Chem. Res. 14 (1981) 109. (b) C.M. Lukehart, Adv. Organomet. Chem. 25 (1986) 45.

[6] D. Steinborn, R. Nünthel, J. Sieler, R. Kempe, Chem. Ber. 126 (1993) 2393.

[7] (a) D. Steinborn, M. Gerisch, F.W. Heinemann, C. Bruhn, Chem. Commun. (Cambridge) (1997) 843. (b) M. Gerisch, C. Bruhn, A. Porzel, D. Steinborn, Eur. J. Inorg. Chem. (1998) 1655. (c) M. Gerisch, C. Bruhn, D. Steinborn, Polyhedron 18 (1999) 1953.

[8] M. Gerisch, F.W. Heinemann, C. Bruhn, J. Scholz, D. Steinborn, Organometallics 18 (1999) 564.

[9] (a) R. Taylor, O. Kennard, J. Am. Chem. Soc. 104 (1982) 5063. (b) C.B. Aakeröy, K.R. Seddon, Z. Naturforsch. 48b (1993) 1023. (c) C.B. Aakeröy, T.A. Evans, K.R. Seddon, I. Pálinkó, New J. Chem. (1999) 145.

[10] W.B. Connick, R.E. Marsh, W.P. Schaefer, H.B. Gray, Inorg. Chem. 36 (1997) 913 and literature cited therein.

[11] V.M. Miskowski, V.H. Houlding, Inorg. Chem. 28 (1989) 1529.

[12] (a) T.W. Thomas, A.E. Underhill, Chem. Soc. Rev. 1 (1972) 99. (b) V.H. Houlding, V.M. Miskowski, Coord. Chem. Rev. 111 (1991) 145.

[13] V.M. Miskowski, V.H. Houlding, C.-M. Che, Y. Wang, Inorg. Chem. 32 (1993) 2518.

[14] G. Israel, F.W. Müller, C. Damm, J. Harenburg, J. Inf. Rec. 23 (1997) 559.

[15] (a) E.W. Colvin, Silicon Reagents in Organic Synthesis, Academic Press, London, 1990. (b) L. Brandsma, Preparative Acetylenic Chemistry, Elsevier, Amsterdam, 1988.

[16] G.M. Sheldrick, SHELXS-86, SHELXL-93, Programs for Crystal Structure Determination, University of Göttingen, Göttingen, 1986, 1993.

[17] M.N. Burnett, C.K. Johnson, ORTEP-III, Oak Ridge Thermal Ellipsoid Plot Program for Crystal Structure Illustrations, Oak Ridge National Laboratory Report ORNL-6895, 1996.